Electronic Supplementary Information (ESI)

Lattice Oxygen of PbO_2 Induces Crystal Facet Dependent Electrochemical Ozone Production

Wenbin Jiang†, Shibin Wang†, Jia Liu†, Haiyang Zheng, Yu Gu, Wenwen Li, Huaijie Shi, Suiqin Li, Xing Zhong, Jianguo Wang**

Institute of Industrial Catalysis, College of Chemical Engineering, State Key Laboratory Breeding Base of Green-Chemical Synthesis Technology, Zhejiang University of Technology, Hangzhou 310032 China.

†W.B. Jiang, S.B. Wang and J. Liu contribute to this work equally

*Correspondence and requests for materials should be addressed to X.Z. (email: zhongx@zjut.edu.cn) or to J.G.W. (email: jgw@zjut.edu.cn).

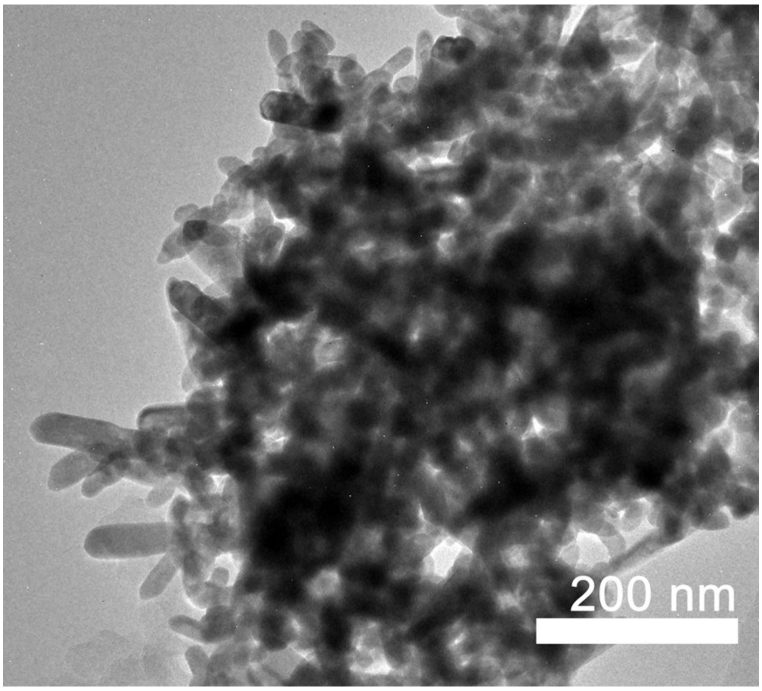

Fig. S1. TEM image of the β-PbO_2-120 NRs.

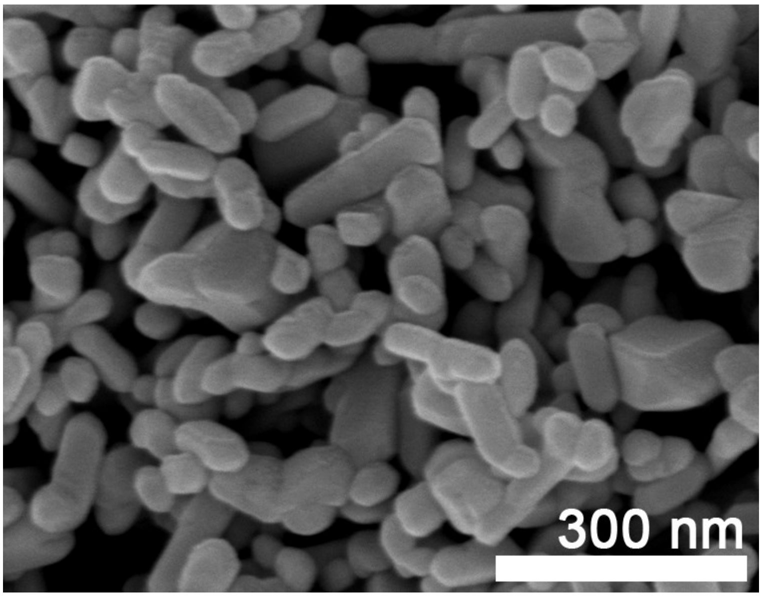

Fig. S2. SEM image of the β-PbO_2-150 NRs.

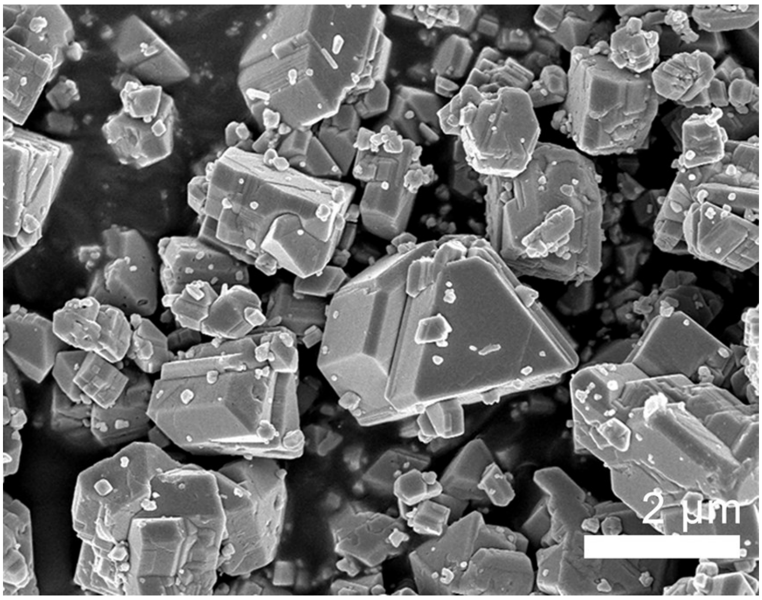

Fig. S3. SEM image of the β-PbO_2-CM.

Table S1. The relative concentration of different Pb species based on XPS of the β-PbO_2-120 NRs, β-PbO_2-150 NRs and the β-PbO_2-CM.

Samples	Relative concentration of different Pb species (area %)	
	Pb^{4+}	Pb^{0}
β-PbO_2 NRs	79.89	20.10
β-PbO_2-150 NRs	79.83	20.17
β-PbO_2-CM	60.40	39.59

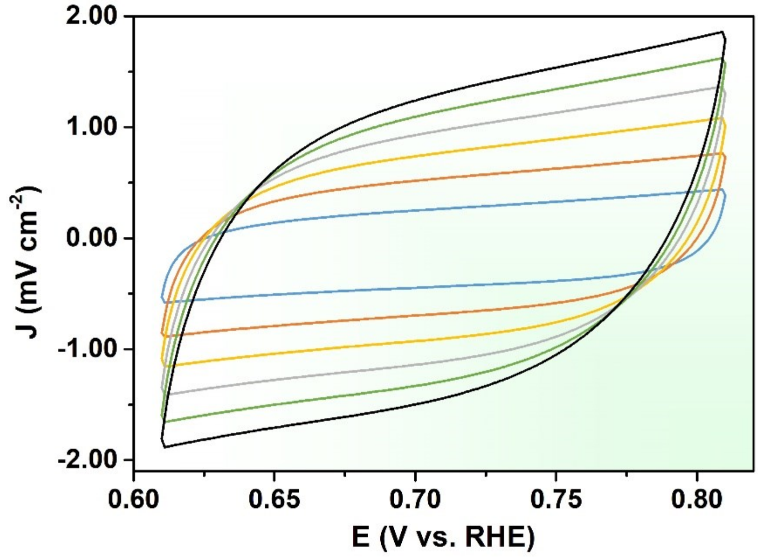

Fig. S4. Cyclic voltammetry curves at various scan rates of the β-PbO_2-120 NRs at various scan rates of 20, 40, 60, 80, 100, and 120 mV/s in saturated K_2SO_4 solution.

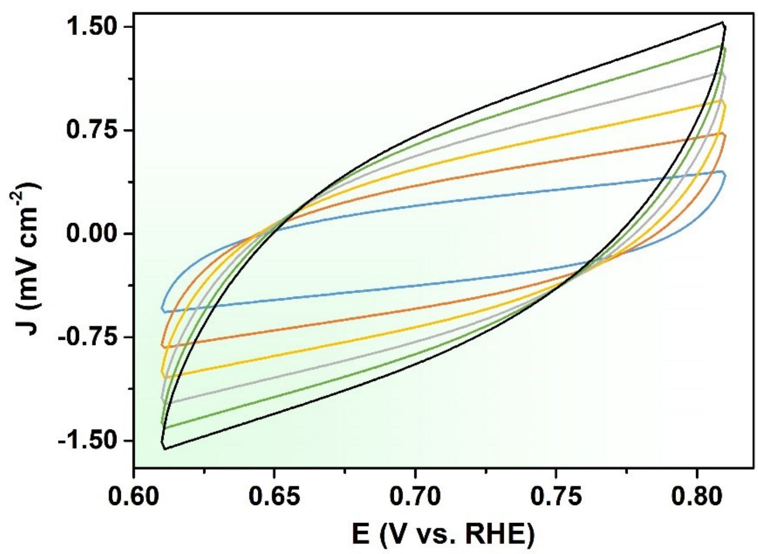

Fig. S5. Cyclic voltammetry curves at various scan rates of the β-PbO_2-150 NRs at various scan rates of 20, 40, 60, 80, 100, and 120 mV/s in saturated K_2SO_4 solution.

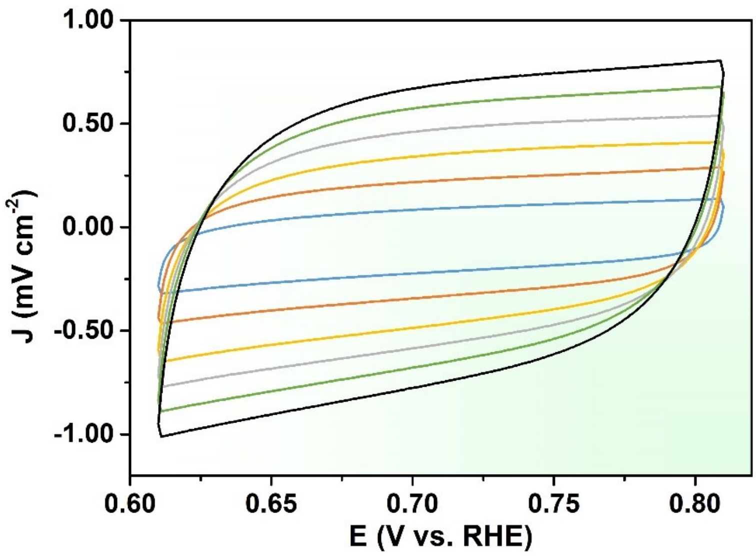

Fig. S6. Cyclic voltammetry curves at various scan rates of the β-PbO_2-CM at various scan rates of 20, 40, 60, 80, 100, and 120 mV/s in saturated K_2SO_4 solution.

Table S2. Comparison of EOP performance for of the β-PbO_2-120 NRs, β-PbO_2-150 NRs and the β-PbO_2-CM..

Catalysts[a)]	**Tafel Slope**[b)] **(mV/dec)**	$J_{0,\ geometric}$[c)] **(mA/cm²)**	C_{dl} **(mF/cm²)**	**Relative surface area**	$J_{0,\ normalized}$ **(mA/cm²)**
β-PbO_2-120 NRs	1791.8	742.3	40.76	1.80	412.4
β-PbO_2-150 NRs	1515.2	411.5	21.22	0.93	440.2
β-PbO_2-CM	1561.4	493.2	22.70	1.00	493.2

a) All the parameters were measured under the same conditions. b) The higher current densities of Tafel slopes were taken to calculate. c) Exchange current densities (J_0) were obtained from Tafel curves by using extrapolation methods.

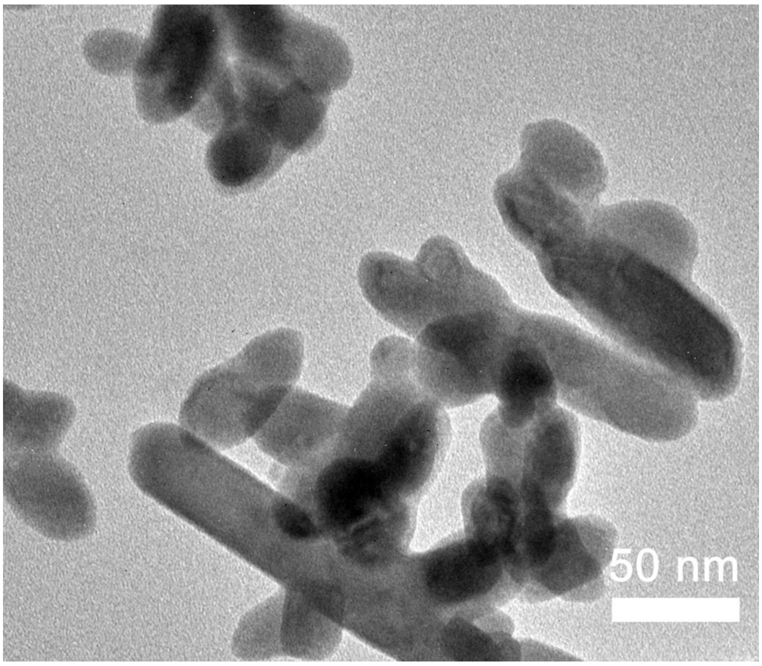

Fig. S7. TEM image of the β-PbO_2-120 NRs after EOP stability test for 50 h in the MEA electrolyzer.

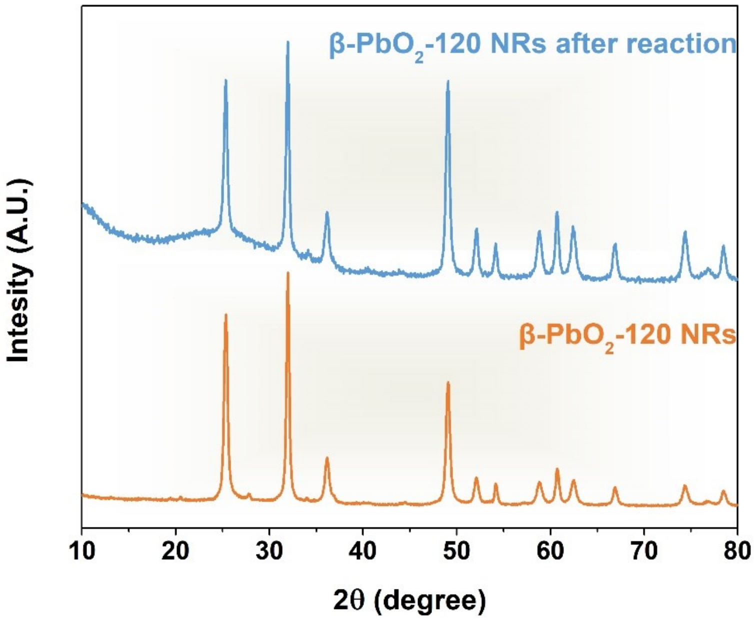

Fig. S8. XRD patterns for the β-PbO_2-120 NRs and the β-PbO_2-120 NRs after EOP stability test for 50 h in the MEA electrolyzer.

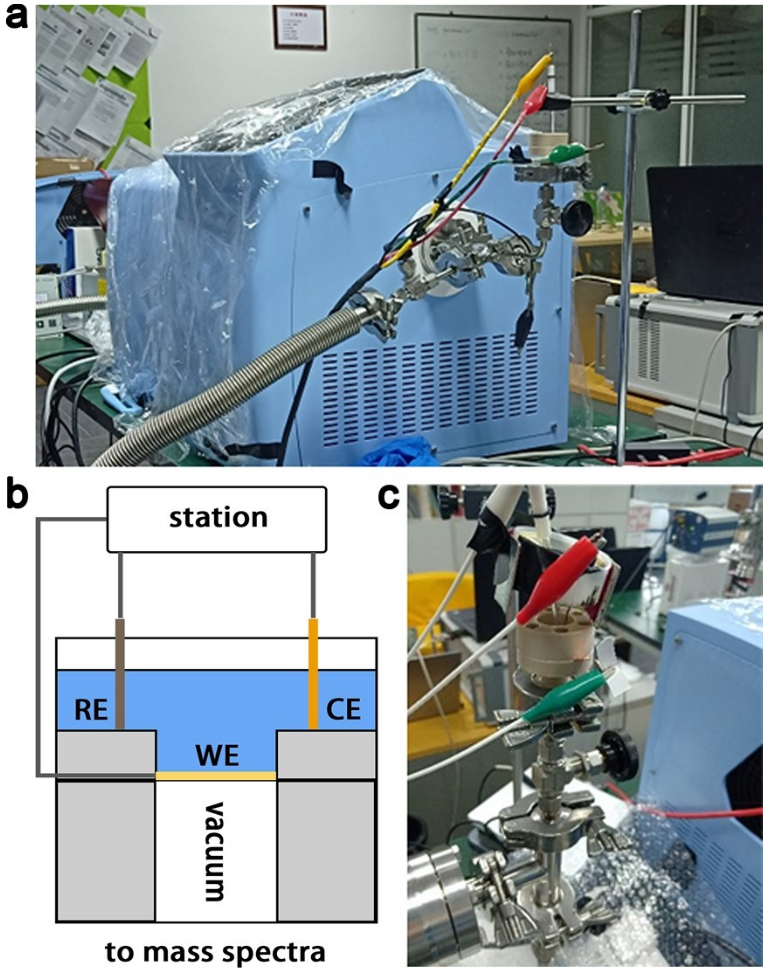

Fig. S9. a) The photograph of the DEMS technique with mass spectra. b**)** The schematic illustration of the DEMS technique. c)The photograph of the electrolysis cell for DMES measurement.

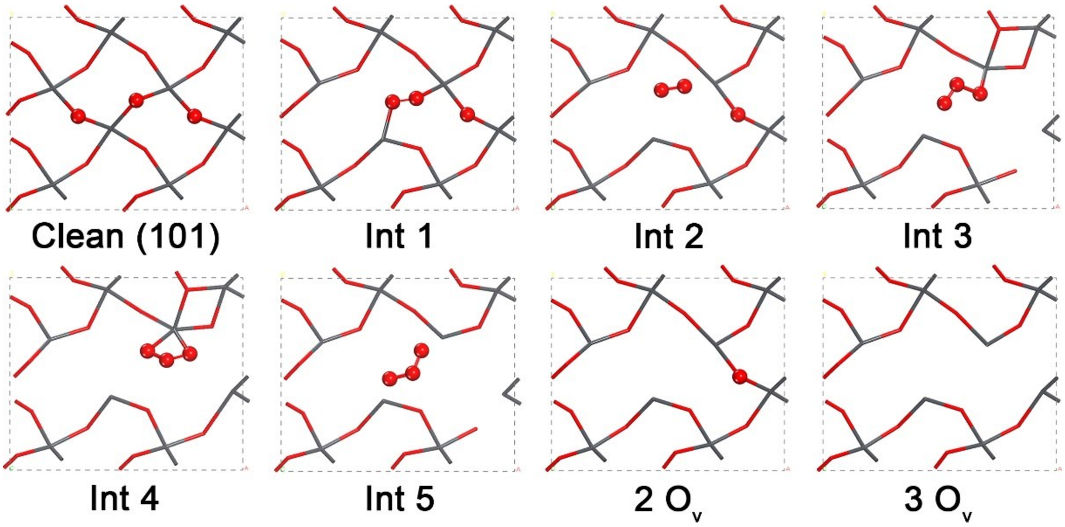

Fig. S10. Optimized structures of the reaction intermediates in surface lattice oxygen coupling to O_2/O_3 on the PbO_2 (101) surface.

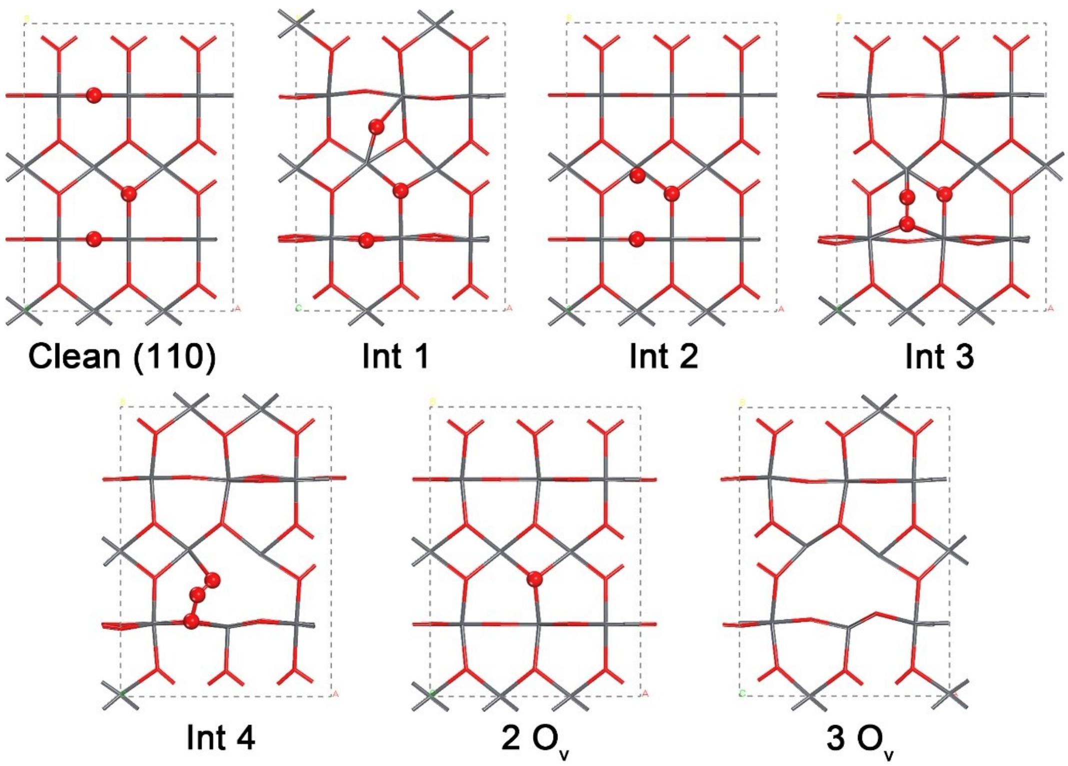

Fig. S11. Optimized structures of the reaction intermediates in surface lattice oxygen coupling to O_2/O_3 on the PbO_2 (110) surface.

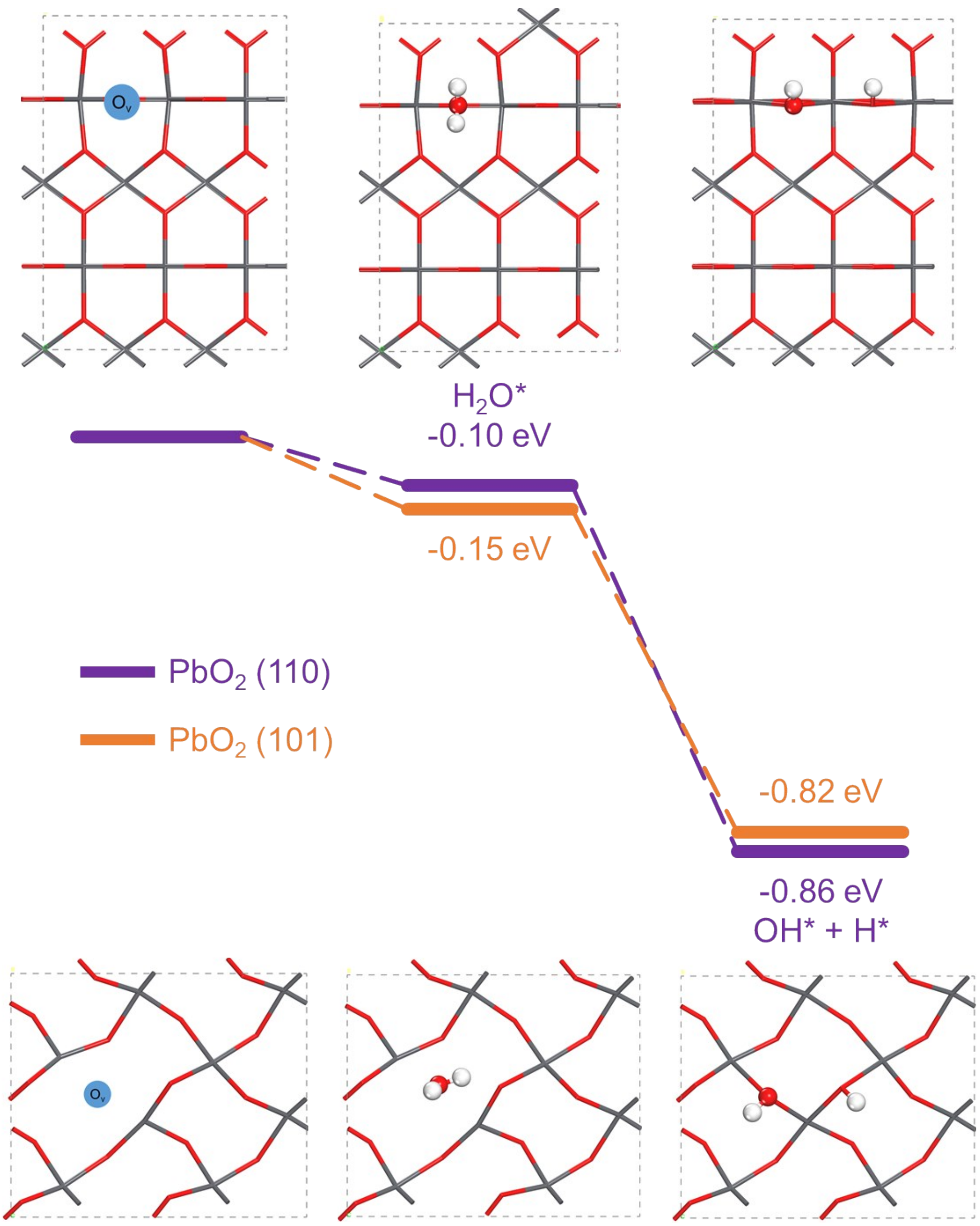

Fig. S12. The free energy diagram (298K) and optimized structures for H_2O adsorption and dissociation on the PbO_2 (101) and the PbO_2 (110) surface.

Table S3. Calculated Gibbs reaction energies (ΔG_r) and energy barriers (ΔG_a) for elementary steps in surface lattice oxygen coupling to O_2/O_3 on the PbO_2 (101) and the PbO_2 (110) surface.

	ΔG_r (eV)	**ΔG_a (eV)**
(110): 3 O_{latt}* → O* (bri) + 2 O_{latt}* + O_v	0.73	−
(110): O* (bri) + 2 O_{latt}* + O_v → O* (top) + 2 O_{latt}* + O_v	0.42	−
(110): O* (top) + 2 O_{latt}* + O_v → O_2* + O_{latt}* + 2 O_v	-1.91	0.11
(110): O_2* + O_{latt}* + 2 O_v → O_3* + 3 O_v	0.19	0.92
(110): O_2* + O_{latt}* + 2 O_v → O_2 (gas) + O_{latt}* + 2 O_v	-1.08	−
(110): O_3* + 3 O_v + 2 O_v → O_3 (gas) + 3 O_v	1.15	−
(101): 3 O_{latt}* → O_2* + O_{latt}* + 2 O_v	-1.20	0.74
(101): O_2* + O_{latt}* + 2 O_v → O_2 (phys) + O_{latt}* + 2 O_v	-0.44	−
(101): O_2 (phys) + O_{latt}* + 2 O_v → O_3* (1) + 3 O_v	-0.05	0.41
(101): O_3* (1) + 3 O_v → O_3* (2) + 3 O_v	-0.17	0.08
(101): O_3* (2) + 3 O_v → O_3 (phys) + 3 O_v	0.47	−
(101): O_3* (phys) + 3 O_v → O_3 (gas) + 3 O_v	-0.16	−
(101): O_2 (phys) + O_{latt}* + 2 O_v → O_2 (gas) + O_{latt}* + 2 O_v	-0.40	−